JOURNAL OF VIROLOGY, Aug. 2006, p. 7522–7534 Vol. 80, No. 15
0022-538X/06/$08.00+0 doi:10.1128/JVI.00241-06

Newcastle Disease Virus Exerts Oncolysis by both Intrinsic and Extrinsic Caspase-Dependent Pathways of Cell Death

Subbiah Elankumaran, Daniel Rockemann, and Siba K. Samal*

Virginia-Maryland Regional College of Veterinary Medicine, University of Maryland, College Park, Maryland 20742

Received 2 February 2006/Accepted 15 May 2006

Newcastle disease virus (NDV), an avian paramyxovirus, is tumor selective and intrinsically oncolytic. Here, we present evidence that genetically modified, recombinant NDV strains are cytotoxic to human tumor cell lines of ecto-, endo-, and mesodermal origin. We show that cytotoxicity against tumor cells is due to multiple caspase-dependent pathways of apoptosis independent of interferon signaling competence. The signaling pathways of NDV-induced, cancer cell-selective apoptosis are not well understood. We demonstrate that NDV triggers apoptosis by activating the mitochondrial/intrinsic pathway and that it acts independently of the death receptor/extrinsic pathway. Caspase-8-methylated SH-SY5Y neuroblastoma cells are as sensitive to NDV as other caspase-8-competent cells. This demonstrates that NDV is likely to act primarily through the mitochondrial death pathway. NDV infection results in the loss of mitochondrial membrane potential and the subsequent release of the mitochondrial protein cytochrome *c*, but the second mitochondrion-derived activator of caspase (Smac/DIABLO) is not released. In addition, we describe early activation of caspase-9 and caspase-3. In contrast, cleavage of caspase-8, which is predominantly activated by the death receptor pathway, is a TNF-related, apoptosis-inducing ligand (TRAIL)-induced late event in NDV-mediated apoptosis of tumor cells. Our data, therefore, indicate that the death signal(s) generated by NDV in tumor cells ultimately converges at the mitochondria and that it acts independently of the death receptor pathway. Our cytotoxicity studies demonstrate that recombinant NDV could be developed as a cancer virotherapy agent, either alone or in combination with therapeutic transgenes. We have also shown that trackable oncolytic NDV could be developed without any reduction in oncolytic efficacy.

Naturally occurring or engineered oncolytic viruses (OVs) are emerging as novel tools for selective growth in and killing of a variety of tumor cells. OVs are multimodality therapeutics that can be engineered to have the tumor specificity of a small molecule, the potent cell killing of a chemotherapeutic, the ability to arouse the host immune system against tumor antigens, and an innate capacity to stimulate the production of host cytokines that have potential anticancer activity (3, 28, 51). Among the OVs, Newcastle disease virus (NDV) is considered to be a very promising oncolytic agent (34–35, 44, 47). NDV has been used in a clinical setting as an experimental oncolytic agent for more than 30 years (10, 36).

NDV contains a single-stranded, negative-sense, nonsegmented RNA genome and belongs to the genus *Avulavirus* in the family *Paramyxoviridae* (37). The genomic RNA is 15,186 nucleotides in length (27) and contains six genes that encode at least seven proteins (50). The envelope of NDV contains two glycoproteins, the hemagglutinin-neuraminidase (HN) and fusion (F) proteins: the HN protein mediates attachment of the virus to the cell, and the F protein mediates fusion of the viral envelope with cellular membranes (8). In common with other paramyxoviruses, NDV produces two additional proteins, V and W, from the P gene by alternative mRNAs that are generated by RNA editing (50).

Although much preclinical work establishing that NDV could serve as a cancer therapeutic has been carried out, the mechanisms governing cytotoxicity remain to be fully characterized. NDV strains are known to evoke cellular apoptosis (30, 58). The reported apoptosis signaling pathways induced by NDV in tumor cells are inconsistent and conflicting. It has been suggested that tumor necrosis factor alpha (TNF-α) might be involved in the tumoricidal activity of NDV-activated murine macrophages and human peripheral blood mononuclear cells (36, 65). It is also claimed that the cell-to-cell contact killing of tumor cells by NDV-stimulated macrophages is mediated by TNF-related, apoptosis-inducing ligand (TRAIL) (58). Most of these studies tested the apoptotic response of NDV-activated human cells on human tumor cells. On the other hand, direct infection studies with NDV strain MTH/68 in PC12 rat pheochromocytoma cells indicated that major mitogen-activated protein kinase pathways (including the stress-inducible c-Jun N-terminal kinase pathway and the p38 pathway) or mechanisms regulated by reactive oxygen species have no role in virus-induced apoptotic cell death (12, 52).

Apoptosis is a multistep, multipathway cell death program that is inherent in every cell of the body. The apoptotic pathways leading to cell death can generally be divided into two nonexclusive signaling cascades involving death receptors (extrinsic pathways) or mitochondria (intrinsic pathway) (21). In both pathways, cysteine aspartyl-specific proteases (caspases) that cleave cellular substrates are activated, and this leads to the biochemical and morphological changes characteristic of apoptosis. The death receptor family (the TNF receptor superfamily) includes CD95 (Fas/APO-1), TNF-R1, DR3, DR4 (TRAIL-R1), and DR5 (TRAIL-R2) receptors (20, 25, 39). Apoptosis initiated via death receptors involves the adaptor molecule Fas-associating protein with a death domain

* Corresponding author. Mailing address: Virginia-Maryland Regional College of Veterinary Medicine, University of Maryland, College Park, MD 20742. Phone: (301) 314-6813. Fax: (301) 314-6855. E-mail: ssamal@umd.edu.

(FADD) and subsequent proximity-induced activation of caspase-8, an initiator caspase (17). Death at the mitochondrial level is initiated by a perturbation of the mitochondrial membrane potential, followed by release of cytochrome *c*, second mitochondrion-derived activator of caspase (Smac) or direct inhibitor of apoptosis binding protein with low pI (DIABLO) (11, 56), apoptosis-inducing factor, and endonuclease G in the cytosol. Cytosolic cytochrome *c* triggers the formation of a multimeric Apaf-1/cytochrome *c*/dATP/procaspase-9 protein complex termed the apoptosome and leads to the activation of caspase-9 (21). Caspase activation and the activity of already active caspases can be inhibited by the inhibitor of apoptosis proteins (IAPs). In turn, IAPs can be inactivated by Smac/DIABLO or Omi/HtrA2, two regulatory proteins that are released from mitochondria. Both the intrinsic and the extrinsic pathways converge on downstream "executioner" caspases, mainly caspase-3 and caspases-6 and -7, which are responsible for the cleavage of structural cytoplasmic and nuclear proteins, with consequent cell collapse and death (46). Activation of the death receptor pathway and that of the mitochondrion-associated death pathway are not mutually exclusive, and these pathways may interact (cross talk) at many levels.

With the availability of the reverse genetics system for NDV, it is now possible to manipulate the genome of NDV, engineer additional genes, and retarget the virus to specific receptors (4, 18, 26). It also affords a viable system for studying the mechanistic basis of oncolysis by NDV. To this end, we tested several recombinant NDVs (rNDVs), with and without transgenes, and studied their mechanisms of apoptotic cell death in a variety of tumor cell lines. This study has incorporated the following NDV strains with different properties: (i) a strain that is low pathogenic to the natural host (chickens) that replicates only in the presence of exogenous trypsin in cell culture, (ii) a low-pathogenic strain with a mutation in the F protein to allow replication in cell culture without exogenous trypsin, (iii) a moderately pathogenic strain with intact interferon (IFN)-antagonistic function, (iv) a moderately pathogenic strain with a defect in IFN antagonism, and (v) a moderately pathogenic strain with an enhanced green fluorescent protein (EGFP) insert. These strains were chosen to detect the differences in cell death pathways induced by lowly pathogenic and moderately pathogenic NDV strains in tumor cells. The IFN-sensitive virus lacks the expression of the antiapoptotic and IFN-antagonistic V protein (19, 42) and replicates only in cells that lack a functional IFN system. The rNDV that expresses EGFP was used to prove that oncolytic rNDV is a trackable virus in vivo and could be exploited to study the mechanism of cell death in vitro.

We found that rNDV mediates oncolysis by the direct induction of apoptosis through multiple caspase-dependent and interferon-independent pathways. We demonstrate here that NDV acts independently of death receptor signaling to induce apoptosis. NDV primarily triggers the activation of the intrinsic mitochondrial death pathway, leading to programmed cell death. Additionally, we have demonstrated that engineering a reporter gene in rNDV to track the virus in vivo does not compromise oncolytic efficacy and can serve as an aid to understanding the mechanistic basis of oncolysis. We have also shown that IFN-sensitive rNDV that replicates in tumor cells, but not in normal cells, is a better oncolytic agent than its parental type.

MATERIALS AND METHODS

Cells. DF1 chicken embryo fibroblast, HeLa, HEpG2, CaCo2, and HuTu80 cells were grown in Dulbecco's modified Eagle's medium (DMEM) with 10% fetal calf serum (FCS), 100 μg/ml penicillin, and 0.1 μg/ml streptomycin (Invitrogen, Grand Island, NY). T84 colon cancer and SH-SY5Y neuroblastoma cells were grown in a 1:1 mixture of DMEM and Ham's F12 medium with 10% FCS and antibiotics. THP-1, CCRF-CEM, PC3, SW 620, MCF-7, CoLo 205, HT29, and HT1080 cells were grown in RPMI 1640 medium supplemented with 10% FCS and antibiotics. The cells were grown at 37°C with 5% CO_2 in a humidified incubator.

Viruses. The plasmid pNDVfl expressing the full-length antigenome of moderately pathogenic NDV strain Beaudette C (BC) and avirulent NDV strain LaSota have been described previously (18, 26) and were used to construct mutants, chimeric viruses, or viruses with additional transgenes. The construction and recovery of the P gene editing mutant (rBC-Edit), recombinant LaSota (rLaSota), and recombinant LaSota with a Virulent Fusion protein cleavage site (rLaSota V.F.) have been described in detail elsewhere (18–19, 41). The plasmid pNDVfl expressing the full-length antigenome of NDV Beaudette C was used to construct the P gene editing mutant. The AscI-SacII fragment containing the P gene editing site from pNDVfl was subcloned into pGEM-7Z (+) (Promega, Madison, Wis.) between XbaI and HindIII by using a specific primer pair with XbaI and HindIII site overhangs. Mutations were introduced into the P gene editing site by PCR using a phosphorylated primer pair to amplify the plasmid pGEM-7Z (+) containing the AscI-SacII insert. The primer pair P3 (5′-^{2282}gA AaGGCCTATGGTCGAGCCCCCAAG^{2307}-3′; lowercase nucleotides indicate mutations) and P4 (5′-^{2281}TTAGCATTGGACGATTTATTGCTGAGC^{2255}-3′) was used to introduce two nucleotide changes to disrupt the P gene editing site. The mutations introduced were silent with regard to the P reading frame. The mutated AscI and SacII fragments were excised to replace the corresponding counterpart in pNDVfl. Recombinant BC-EGFP (rBC-EGFP) was constructed by inserting an extra cistron-encoding EGFP between the P and M gene sequences. Briefly, by site-directed mutagenesis, an XbaI site was created in the noncoding region of the P gene in the SacII-NotI fragment of the NDV antigenome. Subsequently, the EGFP coding sequence was amplified from pEGFP (Clontech, Mountain View, CA) by PCR with an XbaI overhang at both ends and with authentic NDV gene start and gene stop sequences. The EGFP cistron was digested with XbaI and cloned into the SacII-NotI subclone. The plasmid pBCEGFP was constructed by reinserting the SacII-NotI fragment into the plasmid pNDVfl. The presence of the EGFP gene was confirmed by sequencing the respective full-length clone. The rescue procedure for obtaining the recombinant viruses from the infectious full-length clones of NDV has been described in detail previously (18, 26). Briefly, HEp-2 cells at 80 to 90% confluence in a six-well plate were infected with vaccinia MVA-T7 virus at 1 focus-forming unit per cell. The cells were then transfected with the three expression plasmids encoding the NP, P, and L proteins of NDV strain Beaudette C or LaSota and a fourth plasmid containing the mutated NDV cDNA. Three days after transfection, the cell culture supernatant was harvested, briefly clarified, and then used to infect fresh HEp-2 cells. Three days later, the supernatant was harvested and passed on to the DF1 cells until virus-specific cytopathic effect (CPE) appeared. The recovered viruses were plaque purified on DF1 cells and propagated in 9-day-old embryonated specific-pathogen-free chicken eggs for use as virus stocks.

Western blot analysis. Chicken embryo fibroblast (DF1) cells or tumor cell lines in 10-cm dishes were infected with rNDV at a multiplicity of infection (MOI) of 5. One hour after infection, the media were removed and replaced with OptiMEM for the duration of the experiment. Virus-infected cells were harvested at the indicated times, pelleted by centrifugation, washed with ice-cold phosphate-buffered saline, and lysed by sonication in 150 μl of lysis buffer (1% NP-40, 0.15 M NaCl, 5.0 mM EDTA, 0.01 M Tris [pH 8.0], 1.0 mM phenylmethylsulfonyl fluoride, 0.02 mg/ml leupeptin, and 0.02 mg/ml trypsin inhibitor). Lysates were cleared by centrifugation (15,000 × *g*, 2 min), normalized for protein content, mixed 1:1 with sample buffer, boiled for 5 min, and stored at −70°C. To prepare mitochondrion-free extracts, cells were pelleted, washed twice in ice-cold phosphate-buffered saline, and incubated on ice for 30 min in buffer containing 220 mM mannitol, 68 mM sucrose, 50 mM piperazine-*N*,*N*′-bis(2-ethanesulfonic acid) (PIPES)-KOH (pH 7.4), 50 mM KCl, 5 mM EDTA, 2 mM $MgCl_2$, 1 mM dithiothreitol, and protease inhibitors cocktail (Roche, Indianapolis, IN). Lysates were centrifuged at 14,000 × *g* for 15 min at 4°C to remove debris. Supernatants and mitochondrial pellets were prepared for electrophoresis as described above. Proteins were separated by 10% sodium dodecyl sulfate-

polyacrylamide gel electrophoresis and transferred to a nitrocellulose membrane for immunoblotting. Blots were then probed with the specific antibodies. Proteins were visualized using the trimethylbenzidine membrane substrate (Kirkegaard and Perry Laboratories, Gaithersburg, MD). The following antibodies were used for immunoblotting: Stat1α (sc-345; Santa Cruz Biotechnology, Inc., Santa Cruz, CA), Stat2 (sc-476; Santa Cruz), monoclonal anti-human TRAIL/TNFSF10 (MAB687; R&D Systems, Minneapolis, MN), anti-cytochrome *c* (sc-13561; Santa Cruz), NDV-MCA (monoclonal antibody cocktail directed against the NDV HN protein) (31), and actin (sc-8432; Santa Cruz).

WST-1 assay. A colorimetric assay for analyzing cell viability is based on the cleavage of the tetrazolium salt WST-1 by mitochondrial dehydrogenases. In each experiment, the test cell line was seeded into 96-well plates at 1×10^4 cells/well in growth medium (DMEM + 10% FCS or RPMI + 10% FCS; Invitrogen). Following overnight incubation (37°C and 5% CO_2), media were removed by aspiration, and to each well 20 μl of virus-containing OptiMEM (Invitrogen) was added, with the MOI ranging in 10-fold increments from 0.01 to 10 or with no virus for the negative control medium. Each virus dose was tested in replicates of six. After 60 min of incubation to allow virus attachment, 80 μl of growth medium was added to each well, and the plates were incubated for another 48 h. Cell viability was measured by adding 10 μl of WST-1 reagent (Roche)/well. An expansion of the number of viable cells increases the overall activity of mitochondrial dehydrogenases. This leads to an increase in the amount of formazan dye that is formed and directly correlates with the number of metabolically active cells in the culture. The formazan dye produced by metabolically active cells was quantified 2 h after the addition of WST-1 reagent by measurement in a scanning multiwell spectrophotometer at 450 nm. Background absorbance was subtracted using the control medium and WST-1 reagent.

Annexin V staining and DNA laddering. Nuclei of rNDV-infected tumor cells were visualized after cell fixation in 4% paraformaldehyde, permeabilization with a 90/10 mixture of ice-cold acetone and water, and DNA staining with 1.0 μg of 4′,6′-diaimidino-2-phenylindole (DAPI) (Sigma-Aldrich, St. Louis, Missouri). Externalization of phosphatidyl serine from the inner to the outer leaflet of the cell membrane in rNDV-infected tumor cells was detected using an annexin V-fluorescein isothiocyanate kit (BD Biosciences, San Jose, CA) per the manufacturer's instructions at 6 and 14 h postinfection (p.i.). Propidium iodide was used as the vital dye to differentiate live, dead, and apoptotic cells by epifluorescence microscopy (Axiovert 200; Carl Zeiss, Thornwood, NY). Intranucleosomal DNA fragmentation in infected cells was detected by using an apoptotic DNA ladder kit (Roche). A kinetic assay of DNA fragmentation was performed in HuTu80 cells at 8, 10, 12, 24, and 48 h p.i.

TNF-α and TRAIL. TNF-α production by rNDV in SV-HUC1 and tumor cell lines was tested at 48 h p.i. using a human TNF-α Quantikine enzyme-linked immunosorbent assay (ELISA) kit (HSTA00C; R&D Systems). The time course of TNF-α induction by rNDV strains (MOI, 10) was monitored in HuTu80 cells at 6, 10, 12, 20, 24, 48, and 72 h p.i. by using the above-mentioned ELISA kit. A TRAIL ActivELISA kit (Imgenex, San Diego, CA) was used to detect the soluble form of TRAIL (sTRAIL) by a sandwich ELISA protocol according to the manufacturer's recommendations. Culture supernatants (48 h p.i.) from rNDV-infected (MOI, 10) DF1 or tumor cells or standard dilutions of recombinant sTRAIL were tested in triplicate using a TRAIL ActivELISA kit. sTRAIL was captured on the microtiter plate by using an anti-TRAIL antibody. The amount of bound TRAIL was then detected by TRAIL-specific detecting antibody, followed by incubation with alkaline phosphatase-conjugated secondary antibody and color reaction with *p*-nitrophenyl phosphate. Optical density was measured at 405 nm and compared with those for the standard dilutions.

Caspase assay. ApoAlert Caspase fluorescent assay kits (BD Biosciences) for caspase-3, caspase-8, and caspase-9 were employed to detect the activation of different caspases in infected cell lysates. DF1 cells and various tumor cell lines were infected with rNDV strains (MOI, 10), harvested at 48 h p.i., and tested for activated caspases using fluorogenic substrates per the manufacturer's instructions. In time course experiments with HuTu80 cells, 1×10^6 cells/time point were used. Cells were centrifuged at $200 \times g$, supernatants were removed, and the cell pellets were frozen at −70°C until cells from all of the time points were collected. Assays were performed in 96-well plates and analyzed using a fluorescent plate reader (PerkinElmer, Boston, MA). The caspase-3 and caspase-8 fluorescent assay kits detect the emission shift of 7-amino-4-trifluoromethyl coumarin (AFC). The AFC-substrate conjugate usually emits blue light (λ_{max} = 400 nm); however, cleavage of the substrate by the appropriate caspase liberates AFC, which fluoresces yellow-green (λ_{max} = 505 nm). Similarly, the caspase-9 fluorescent assay kit detects the emission shift of 7-amino-4-methyl coumarin (AMC). The LEHD-AMC conjugate emits light in the UV range (λ_{max} = 380 nm); however, free AMC fluoresces blue-green at 440 nm upon liberation by caspase-9. The amount of fluorescence detected is directly proportional to the amount of caspase activity. Results of all experiments are reported as means + standard errors of the mean (SEM).

TABLE 1. Recombinant Newcastle disease virus strains used in this study

Virus[a]	Additional, replaced, or mutated gene
Recombinant LaSota	None
Recombinant LaSota V.F.	Virulent Fusion (V.F.) protein cleavage site
Recombinant Beaudette C	None
Recombinant Beaudette C-Edit	V protein editing site mutant
Recombinant Beaudette C-EGFP	Enhanced green fluorescent protein (EGFP)

[a] All viruses were recovered entirely from cloned cDNAs of their respective antigenome by our established reverse genetics techniques.

Caspase inhibition. The selective inhibitors acetyl-Asp-Glu-Val-Asp-aldehyde (Ac-DEVD-CHO; inhibitor of caspase-3, -7, and -8), benzyloxycarbonyl-Ile-Glu-Thr-Asp-fluoromethylketone (Z-IETD-FMK; inhibitor of caspase-6, -8, -9, and -10), and acetyl-Leu-Glu-His-Asp-aldehyde (Ac-LEHD-CHO; inhibitor of caspase-9) were used for caspase inhibition experiments. For apoptosis inhibition assays, HuTu80 cells were incubated with 600 μM Ac-DEVD-CHO, 600 μM Ac-LEHD-CHO, or 120 μM Z-IETD-FMK for 3 h or with 100 μM benzyloxycarbonyl-Val-Ala-Asp-fluoromethylketone (Z-VAD-FMK) for 1 h prior to infection with rBC-EGFP (MOI of 1), rLaSota V.F., rBC, or rBC-Edit viruses. Control cultures were treated with the appropriate amount of dimethyl sulfoxide (0.1%, final concentration), used as a solvent for peptide inhibitors. After virus adsorption for 1 h, the media were removed and replaced with OptiMEM. The infected cells were monitored for either EGFP expression or CPE and virus production at 6, 8, 10, 12, 14, 16, 20, 24, 38, 48, and 72 h p.i. Apoptosis induction in these cells was evaluated using an apoptotic DNA ladder kit (Roche) for intranucleosomal DNA fragmentation at the time points indicated above.

Mitochondrial membrane stability assay. To detect mitochondrial membrane integrity, tumor cells were cultured on 24-well cell culture plates. Fifteen minutes before fixation, the MitoTracker Red (750 nM) (CMX-Ros; Molecular Probes, Eugene, OR) dye was added to the culture medium. Accumulation of the dye was allowed to occur for 20 min at 37°C. Then, the cells were fixed with 4% paraformaldehyde for 15 min and permeabilized with a 90/10 acetone-water solution during 2 min at −20°C. After three washes, cells were labeled with DAPI, mounted in buffered glycerol, and analyzed by epifluorescence microscopy. MitoTracker Red fluorescence was induced by illumination at 543 nm and was detected using a 560-nm long pass filter.

RESULTS

Rescue of Newcastle disease viruses from cloned cDNAs and expression vectors. By reverse genetics technology, we have recovered several rNDVs expressing additional genes as transcriptional units (18, 26), including one carrying EGFP for this study. The recombinant viruses used in this study are listed in Table 1. The recovered recombinant viruses exhibited all of the biological phenotypes of their parental natural isolates. The rBC-EGFP virus stably expressed EGFP even after 10 passages in 9- to 11-day-old embryonated chicken eggs and 15 passages in DF1 cells.

Recombinant NDV strains are highly lytic for members of the National Cancer Institute panel and other cancer cell lines. To assess the oncolytic properties of the rNDV strains, representative cell lines from the NCI-60 human tumor cell panel and other tumor cell lines (14 cell lines from a spectrum of malignancies) were infected with either rLaSota, rLaSota V.F., rBC, rBC-EGFP, or rBC-Edit viruses and assayed for metabolic cell death by the WST-1 assay 48 h later. The rNDVs were able to infect and induce cytolysis in a wide range of

TABLE 2. Recombinant NDV strains are highly lytic to tumor cells in vitro[c]

Cell line	rLaSota[a]		rLaSota V.F.[a]		rBC[a]		rBC-EGFP[a]		rBC-Edit[a]	
	Sensitivity[b] (%)	MOI	Sensitivity (%)	MOI	Sensitivity (%)	MOI	Sensitivity (%)	MOI	Sensitivity (%)	MOI
THP-1	0	>10	100	0.0001	100	0.003	100	0.001	100	0.04
CCRF-CEM	0	>10	100	0.283	0	>10	0	>10	0	>10
Leukemia cell lines	**0**	**>10**	**100 (2/2)**	**0.142**	**50 (1/2)**	**0.003**	**50 (1/2)**	**0.001**	**50 (1/2)**	**0.04**
Prostate cancer (PC3)	0	>10	100 (1/1)	0.0005	100 (1/1)	0.0001	100 (1/1)	0.01	100 (1/1)	0.0019
HT1080	0	>10	100 (1/1)	3.5562	100 (1/1)	0.02	100 (1/1)	0.01	0	>10
HuTu80	0	>10	100 (1/1)	0.21725	100 (1/1)	0.007	100 (1/1)	0.01	100 (1/1)	0.019
Cervical cancer (HeLa)	100	10	100 (1/1)	0.01	100 (1/1)	0.72	100 (1/1)	1.0	100 (1/1)	0.007
Liver cancer (HEpG2)	100	1.0	100 (1/1)	0.0164	100 (1/1)	0.019	100 (1/1)	0.1	100 (1/1)	0.0022
Caco-2	0	>10	100	0.0573	0	>10	0	>10	100	0.00004
CoLo 205	0	>10	100	0.0076	0	>10	0	>10	0	>10
SW 620	0	>10	100	3.03	100	0.988	100 (1/1)	1.0	100	1.081
HT29	0	>10	100	4.648	0	>10	0	>10	100	0.0006
T84	0	>10	0	>10	0	>10	0	>10	100	0.0391
Colon cancer cell lines	**0**	**>10**	**80 (4/5)**	**1.9357**	**20 (1/5)**	**0.988**	**20 (1/5)**	**1.0**	**80 (4/5)**	**0.2802**
SH-SY5Y neuroblastoma	0	>10	100	0.002	100	0.0025	100 (1/1)	0.01	100	0.0004
Breast carcinoma (MCF-7)	0	>10	0 (0/1)	>10	0 (0/1)	>10	0 (0/1)	>10	0 (0/1)	>10
All cell lines tested	**14 (2/14)**	**>10**	**86 (12/14)**	**0.84**	**57 (8/14)**	**0.22**	**57 (8/14)**	**0.27**	**71 (10/14)**	**0.12**

[a] In parentheses are numbers of highly susceptible cell lines out of the number of cell lines tested. A cell line was considered highly susceptible if the EC_{50} was ≤MOI of 1 following a 48-h infection. The MOI represents the average EC_{50} (MOI) of susceptible cell lines obtained from two independent experiments. All of the tested viruses are recombinant viruses derived by our established reverse genetics techniques.

[b] The sensitivity is the percentage of cancer cell lines by tumor type deemed highly sensitive to virus-mediated killing.

[c] Boldface type indicates combined results for indicated cell lines.

tumor cell types (Table 2). The rLaSota virus was cytotoxic only to HeLa and HEpG2 cells and required MOIs of 10 and 1.0, respectively, for cytolysis. On the other hand, the rLaSota V.F. virus was cytotoxic (mean 50% effective concentration [EC_{50}] = 0.84) to 12 of the 14 tested cell lines but not cytotoxic to T84 colon cancer cells and MCF-7 breast carcinoma cells, while the IFN-sensitive rBC-Edit virus was cytolytic to 10 out of 14 cell lines (mean EC_{50} = 0.12). The parental rBC and rBC-EGFP viruses were cytolytic to 8 of the 14 tested cell lines (mean EC_{50} = 0.22 and 0.27, respectively). The CPE in rNDV-infected cells were cell-to-cell fusion with syncytium formation, rounding and increased granularity of cells leading to destruction of a monolayer of adherent cells (Fig. 1A to P) or granularity, and cell death in suspension cells such as THP-1 and CCRF-CEM. In SV-HUC1 immortalized human uroepithelial cells, NDV replication was severely restricted (Fig. 1Q), and no CPE was observed up to an MOI of 10. As the rLaSota virus was found to be poorly cytolytic in the WST-1 cytotoxic assay, it was not studied further.

Induction of apoptosis by rNDV mediates cytolysis in tumor cells. To determine the nature of rNDV-induced cytolysis, we examined whether rNDV is oncolytic through direct induction of apoptosis. We infected various tumor cells with rNDV at an MOI of 0.01 and examined for markers of apoptosis, viz., morphological changes by DAPI staining, phosphatidyl serine externalization by annexin V staining, and intranucleosomal DNA fragmentation by DNA laddering techniques. In most cases, rNDV infection led to cell death characterized by several hallmarks of apoptosis, including morphological changes of rounding and refraction, loss of adherence, development of pyknotic nuclei (Fig. 2A), and phosphatidyl serine externalization (Fig. 2B). Apoptosis appeared from 6 h after rNDV infection, since then the cells displayed typical annexin V-positive labeling. DNA laddering was observed in most of the cell lines following infection with rNDV as early as 8 h p.i. (Fig. 2C and D).

NDV induces apoptosis of tumor cells independently of IFN signaling. Many studies have shown that IFN-α activates an apoptotic program in several tumor cell lines and primary tumor cells (7, 45, 48). In order to analyze the role of IFN in NDV-induced apoptosis, we infected cell lines that respond to exogenous or endogenous IFN or those that do not respond to IFN due to specific mutations or defects. Apoptosis was induced in human tumor cells independently of IFN signaling, as we detected apoptosis in IFN-responsive cell lines (e.g., 2fTGH) or IFN-unresponsive cell lines (e.g., PC3 and U3A) (Fig. 2E). Further, most of the tested human tumor cell lines were not able to produce IFN-α after NDV infection but showed NDV-induced apoptosis (data not shown).

Death receptor signaling in tumor cells following NDV infection. To identify the signaling pathways that mediate apoptosis in tumor cells, we examined the role of TNF-α and TRAIL, members of the death receptor pathway, in NDV-induced apoptosis. We found that rNDV induced TNF-α as early as 12 h p.i. and the levels were increasing even at 72 h p.i., irrespective of the strain of NDV (Fig. 3A), in tumor cells. However, the highest levels of soluble TNF-α remained below 1 pg/ml in tumor cell lines and 4 to 6 pg/ml in immortalized SV-HUC1 normal human cells (Fig. 3B). Even at a 6-pg/ml concentration, we did not detect apoptosis in SV-HUC1 cells, which suggests that NDV-induced TNF-α does not necessarily mediate apoptosis. TRAIL is a member of the TNF family and, together with its functional and decoy receptors, comprises one of the death receptor pathways for apoptosis. Soluble TRAIL was detected by ELISA in DF1 cells and in only some of the tumor cell lines (Fig. 3C). In TRAIL-resistant colorectal can-

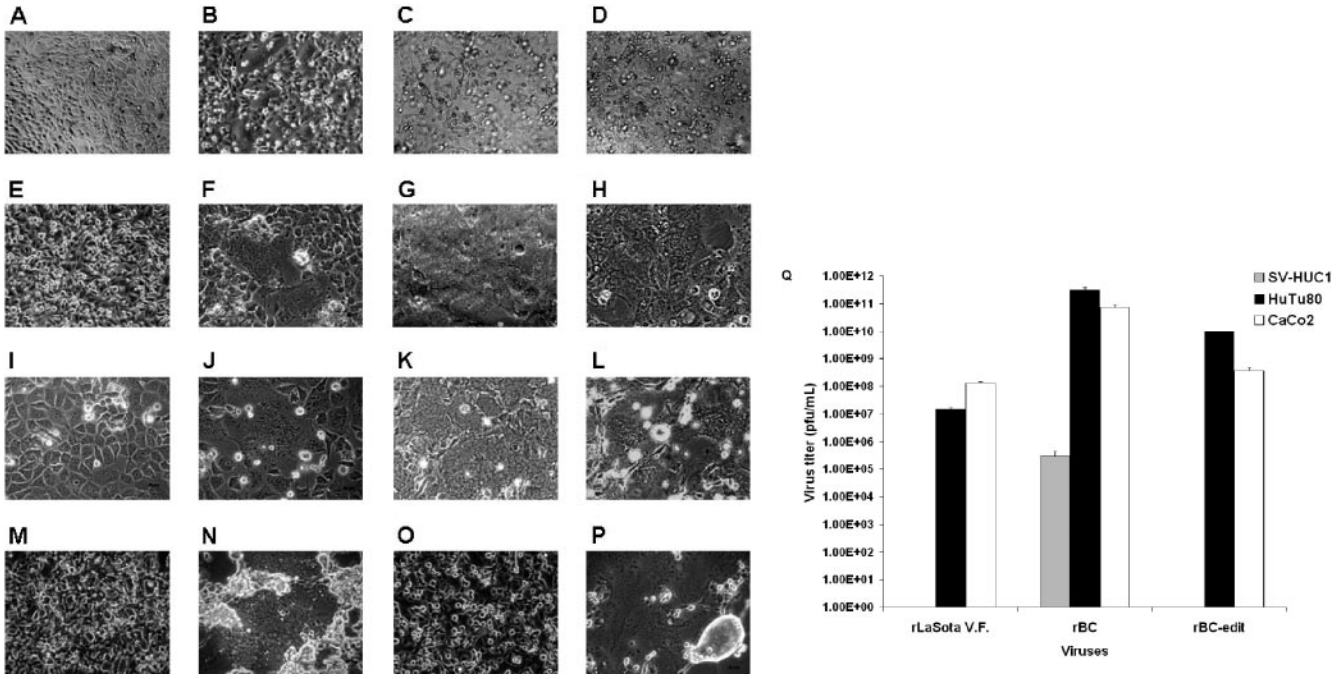

FIG. 1. NDV is cytolytic to human tumor cells and noncytolytic in normal human cells. Shown are CPE induced by rNDV in chicken embryo fibroblast and human tumor cells. DF1 chicken embryo fibroblast cells and human tumor cell lines were either mock infected or infected with rLaSota V.F., rBC, or rBC-Edit strains of NDV at an MOI of 0.01. CPE in the form of cell fusion, syncytium formation, rounding, and destruction of the monolayer in different cells are shown. (A and B) Mock-infected and rBC-Edit-infected HEpG2 cells. (C and D) Mock-infected and rBC-Edit-infected HT1080 cells. (E and F) Mock-infected and rBC-Edit-infected PC3 prostate cancer cells. (G and H) Mock-infected and rBC-Edit-infected CaCo2 colon cancer cells. (I and J) Mock-infected and rBC-Edit-infected HuTu80 intestinal epithelial cells. (K and L) Mock-infected and rBC-Edit-infected DF1 chicken embryo fibroblast cells. (M and N) Mock-infected and rBC-Edit-infected 2fTGH human fibrosarcoma cells. (O and P) Mock-infected and rBC-Edit-infected U3A human fibrosarcoma cells. Magnification, ×40. (Q) SV-HUC1 uroepithelial cells were either mock infected or infected with rLaSota V.F., rBC, or rBC-Edit strains of NDV at MOIs of 0.01, 1.0, or 10. Culture supernatants were assayed for virus content by a plaque assay in DF1 cells at 48 h postinfection, and results of virus titer determination at an MOI of 0.01 were compared with those for viruses assayed under similar conditions in HuTu80 and CaCo2 cells. Results represent mean values + SEM from two independent experiments.

cer cells, such as HT29 and CaCo2 cells, apoptosis was induced by rNDV. Surface expression of TRAIL was detected in many of the cancer cell lines at 48 h p.i., suggesting that human TRAIL is essentially a membrane-bound protein (data not shown). Time course studies by Western blotting in HuTu80 cells indicated that TRAIL expression commenced only at 14 h p.i. (Fig. 3D), which suggests that TRAIL-mediated apoptosis is a late event in NDV-infected cells. Treatment of rBC-EGFP-infected HuTu80 cells with anti-TRAIL antibody (MAB687; R&D Systems) inhibited apoptosis but not the virus replication of rBC-EGFP virus, demonstrable by EGFP expression and viral plaque assay (data not shown).

Caspase-8 is activated but dispensable for apoptosis induction after NDV infection of tumor cells. Death receptor signaling by ligand binding at the cell surface leads to the formation of death-inducing signaling complex and activation of caspase-8. Therefore, we examined the activation of caspase-8 in NDV-infected cells. NDV infection activated caspase-8 in many of the tumor cell lines at 48 h p.i. (Fig. 4A). Caspase-8 was activated independently of IFN responsiveness, indicating that cells respond to NDV with apoptosis either in the presence or in the absence of IFN signaling (59). Caspase-8 was activated in a biphasic manner commencing at 12 h, with peak activation occurring at 32 h p.i. for the rBC virus in HuTu80 cells. Interestingly, rLaSota V.F. and rBC-Edit viruses induced caspase-8 late in the infection cycle (Fig. 4B), following a similar biphasic activation, correlating with the onset of CPE. This biphasic activation indicated that other pathways might amplify caspase-8-induced pathways or that caspase-8 is induced by additional pathways operating independently of death receptor signaling. Further support for this assumption stemmed from the fact that rapid CPE and apoptotic DNA laddering was evident after rNDV infection in TRAIL-sensitive, caspase-8-methylated SH-SY5Y neuroblastoma cells (Fig. 1 and 2D) and TRAIL-resistant CaCo2 and HT29 colon carcinoma cells (Fig. 2E). In CaCo2 and HT29 cells, apoptosis was induced by NDV without any caspase-8 activation. Loss of caspase-8 expression by gene methylation is suggested to be the reason for TRAIL resistance in neuroblastoma cells (53). Caspase-8 activation in neuroblastoma cells commenced only after TRAIL expression was evident in NDV-infected cells (Fig. 4C). Recent evidence suggests that SH-SY5Y neuroblastoma cells become TRAIL sensitive and FADD positive and induce caspase-8 upon stimulation with TRAIL and IFN-γ (22). As our results suggested that caspase-8 is probably not the initiator caspase, we looked for evidence as to whether NDV infection activated intrinsic, mitochondrion-associated

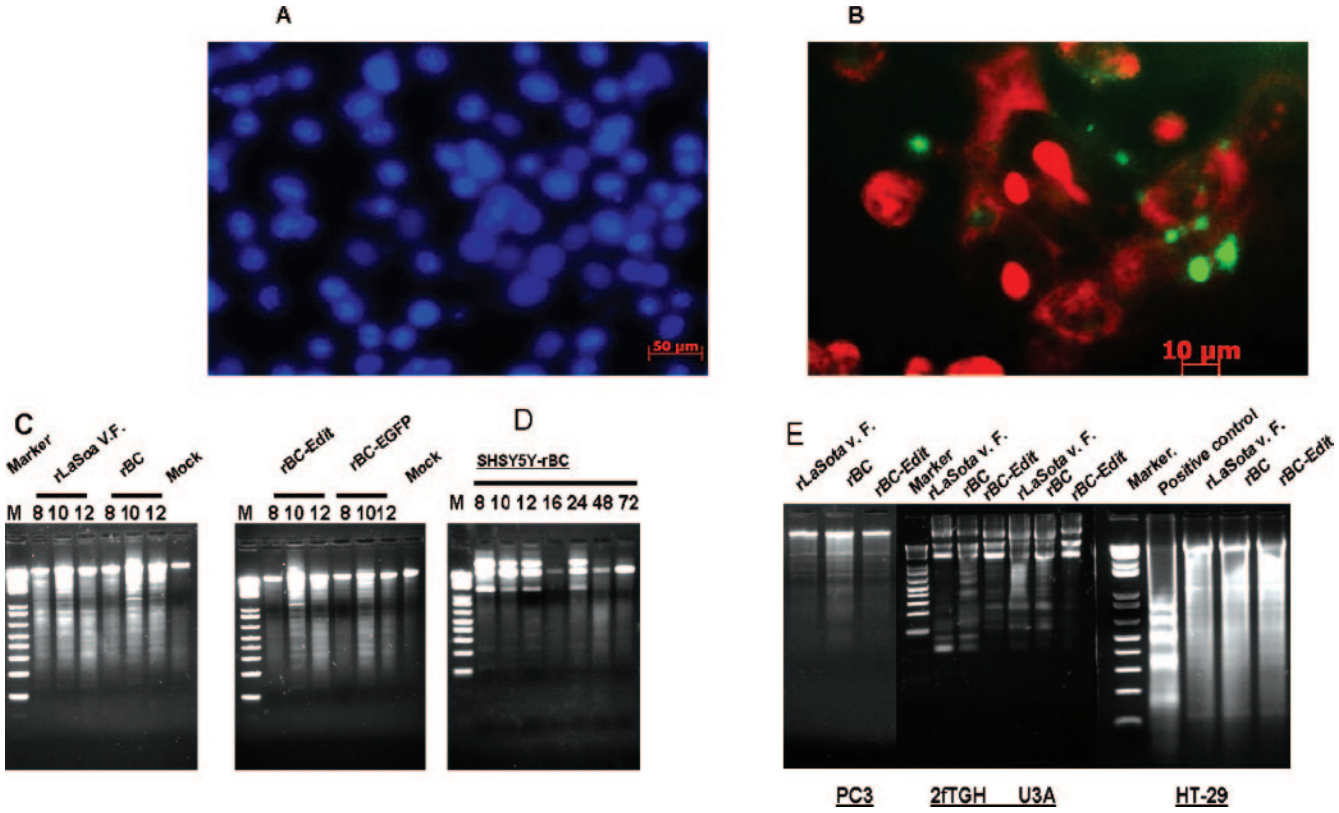

FIG. 2. Morphological features of apoptosis in rNDV-infected human tumor cells. Cells were either mock infected or infected with rLaSota V.F., rBC, rBC-Edit, or rBC-EGFP strains of NDV at an MOI of 0.01. At 6 and 14 h postinfection, apoptotic cell death was visualized by staining the infected cells with DAPI (1 μg/ml). (A) Condensation of chromatin and nuclear fragmentation of rNDV-infected HuTu80 cells. (B) Fluorescein isothiocyanate-annexin V (10 mg/ml) staining of NDV-infected HuTu80 cells. (B) Phosphatidyl serine externalization to the outer leaflet of the infected cell membrane is evident by green fluorescence of the cell membrane. (C) DNA laddering of infected cells was examined by using an apoptotic DNA laddering kit (Roche) per the manufacturer's instructions. Intranucleosomal DNA fragmentation is evident as a laddering pattern of the cellular DNA in rNDV-infected HuTu80 cells at 8, 10, and 12 h postinfection. (D) DNA laddering of SH-SY5Y neuroblastoma cells at 8, 10, and 12 h postinfection. (E) DNA laddering of rNDV-infected PC3, 2fTGH, U3A, and HT29 cells at 12 h postinfection.

apoptotic signaling pathways that may operate earlier than the death receptor pathway.

Mitochondrial membrane potential is not maintained following NDV infection. Cell death at the mitochondrial level is initiated by perturbation of the mitochondrial membrane leading to the release of various proapoptotic factors. To identify the drop in mitochondrial membrane potential ($\Delta\psi_m$), mock- and NDV-infected cells were stained with MitoTracker Red CMX-Ros dye. The CMX-Ros dye is taken up only by actively respiring mitochondria with intact $\Delta\psi_m$. The DNA-binding DAPI fluorophore was then used to delineate the nuclear morphology. NDV-infected cells which had a disruption of the $\Delta\psi_m$ and were undergoing apoptosis were detected by the diffuse cytoplasmic pattern of CMX-Ros (Fig. 5A to I) with condensed chromatin. Cells with intact mitochondrial transmembrane potential displayed punctate staining with CMX-Ros (Fig. 5J to L). Following a drop of $\Delta\psi_m$, cytochrome *c* can be released from mitochondria through the opened mitochondrial pores. Therefore, we investigated the localization of cytochrome *c* after NDV infection. Mitochondrial and cytosolic extracts from mock- and virus-infected cells were prepared by subcellular fractionation and analyzed by Western blotting. In NDV-infected cells, the level of cytochrome *c* in cytosol increased twofold compared to the level observed in mock-infected cells (data not shown). These results indicate that the intrinsic mitochondrial pathway is initiated after infection with NDV.

Smac/DIABLO is not released from the mitochondria following NDV infection. Inhibitor of apoptosis proteins (IAPs) inhibit the enzymatic activity of caspases (55). IAP-mediated inhibition of apoptosis is countered by Smac/DIABLO, and Smac protein is secreted from mitochondria into the cytosol during apoptosis (11, 56). Synthetic Smac-mimicking molecules have been shown to potentiate TRAIL- and TNF-α-mediated cell death (14, 32). We therefore examined the secretion of Smac into the cytosol after infecting HuTu80 cells with rNDV. Mitochondrion-free lysates were prepared from both mock- and NDV-infected cells at specified time points and analyzed by Western blotting for the presence of cytosolic Smac/DIABLO. We were not able to detect Smac expression in rNDV-infected cells at various time points up to 48 h p.i. in HuTu80 cells.

Caspase-9 is activated early after NDV infection. In the cytosol, cytochrome *c* forms an apoptosome with Apaf-1 and procaspase-9, leading to the activation of caspase-9. Caspase-9 was found to be activated by a fluorogenic substrate assay in

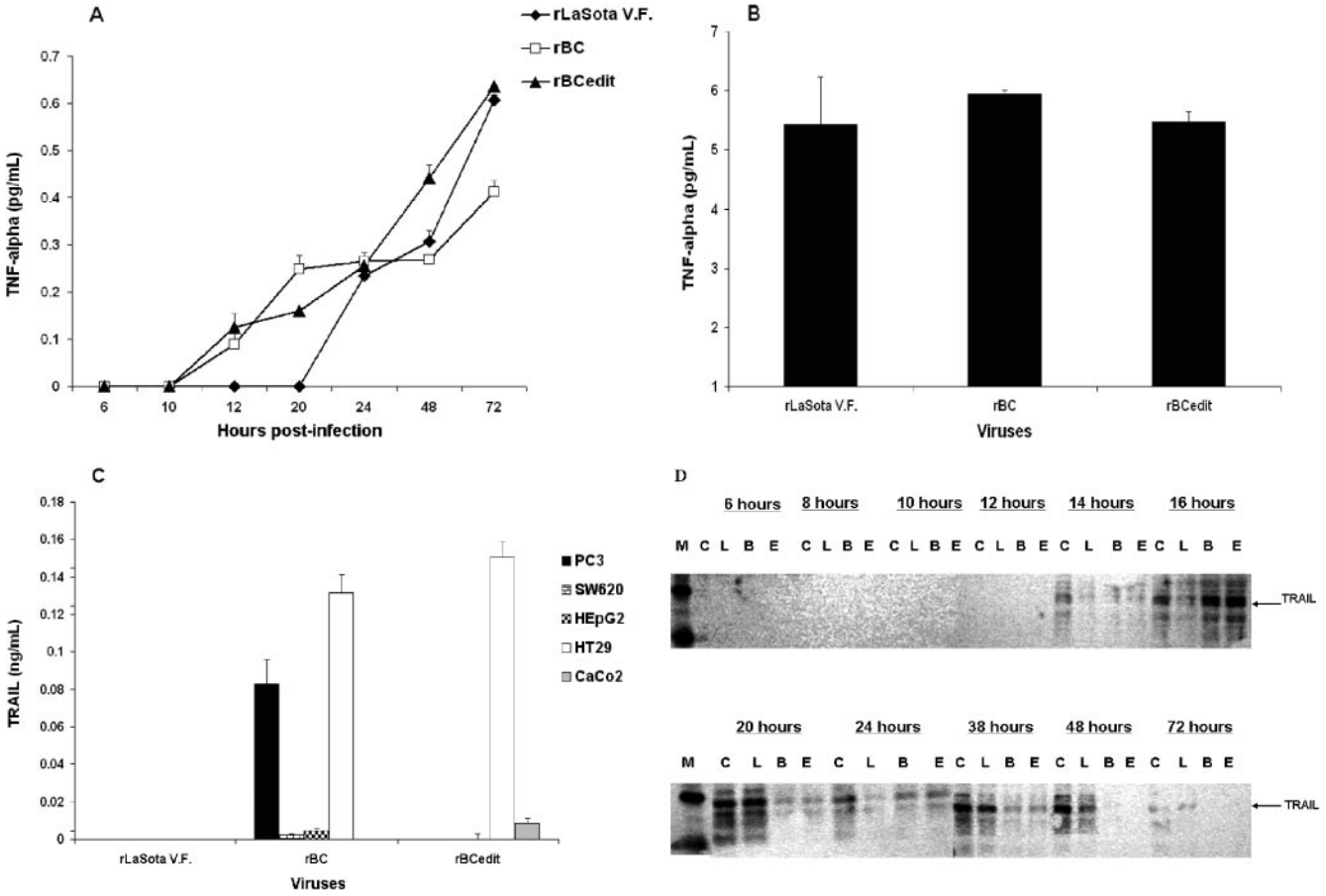

FIG. 3. Apoptotic signaling in rNDV-infected cells. DF1, SV-HUC1, and human tumor cells were either mock infected or infected with rLaSota V.F., rBC, or rBC-Edit strains of NDV at an MOI of 0.01. Culture supernatants were assayed by ELISA for TNF-α production at 48 h postinfection in HuTu80 cells (A) and SV-HUC1 cells (B). Soluble TRAIL expression was assayed by ELISA in various tumor cells at 48 h postinfection (C), and surface expression of TRAIL was examined in HuTu80 cells by immunoblotting with anti-TRAIL antibody at the indicated times postinfection (D). C, mock infected; L, rLaSota V.F. infected; B, rBC infected; E, rBC-Edit infected; M, molecular weight marker. ELISA results represent mean values + SEM from two independent experiments.

most of the tested cell lines (Fig. 6A) after rNDV infection. Significant levels of caspase-9 were induced as early as 6 h p.i. in HuTu80 cells, and caspase-9 also followed a biphasic pattern of activation (Fig. 6B). rLaSota V.F. and rBC-Edit viruses initiated low levels of caspase-9 between 8 and 10 h p.i. followed by another wave of significant induction after 48 h p.i. Similarly, in SH-SY5Y neuroblastoma cells, caspase-9 activation occurred by 12 h after infection with rNDV (Fig. 6C). These results suggest that apoptosis in NDV-infected tumor cells probably commences intrinsically through the double-stranded RNA intermediates and possibly through endoplasmic reticulum stress, leading to mitochondrial membrane destabilization and caspase-9 activation.

Effector caspase activation. Having shown that NDV infection resulted in the activation of both death receptor and mitochondrion-associated pathways, we tested the activation of caspase-3. As shown in Fig. 7A, caspase-3 activation was detected by a fluorogenic substrate assay in many of the cell lines associated with apoptosis. Caspase-3 followed a biphasic activation similar to that of caspase-9 (Fig. 7B). In caspase-3 null MCF-7 breast cancer cells, rNDV strains replicated, although at reduced efficiency, but failed to exert cytolysis ($EC_{50} > 10$), consistent with the idea that caspase-mediated cell death is the predominant mechanism of oncolysis by NDV. In caspase-8-methylated SH-SY5Y neuroblastoma cells, caspase-3 was detected as early as 8 h p.i., which indicates that other initiator pathways are involved in effector caspase activation (Fig. 7C). IFN-sensitive rBC-Edit virus induced caspase-3 in HuTu80 cells at 32 h p.i., while it induced caspase-9 as early as 10 h p.i. but caspase-8 only at 48 h p.i., reinforcing the view that intrinsic apoptotic pathways operate early in NDV-infected cells (Fig. 7B). Classically, caspase-8 has been viewed as an initiator caspase involved in death receptor signaling (62). However, our results demonstrated that caspase-8 was activated only after caspase-9 and caspase-3 were activated. This time course suggested that caspase-8 was not the primary initiator caspase involved in NDV-mediated apoptosis. These results also suggest that caspase-8 activation probably occurs as an indirect effect of activation of caspase-9 and caspase-3 (61) or through the death receptor pathway late in the infection. It is probable that other initiator caspases might be involved, depending on the cell type and virus strain in effector caspase activation.

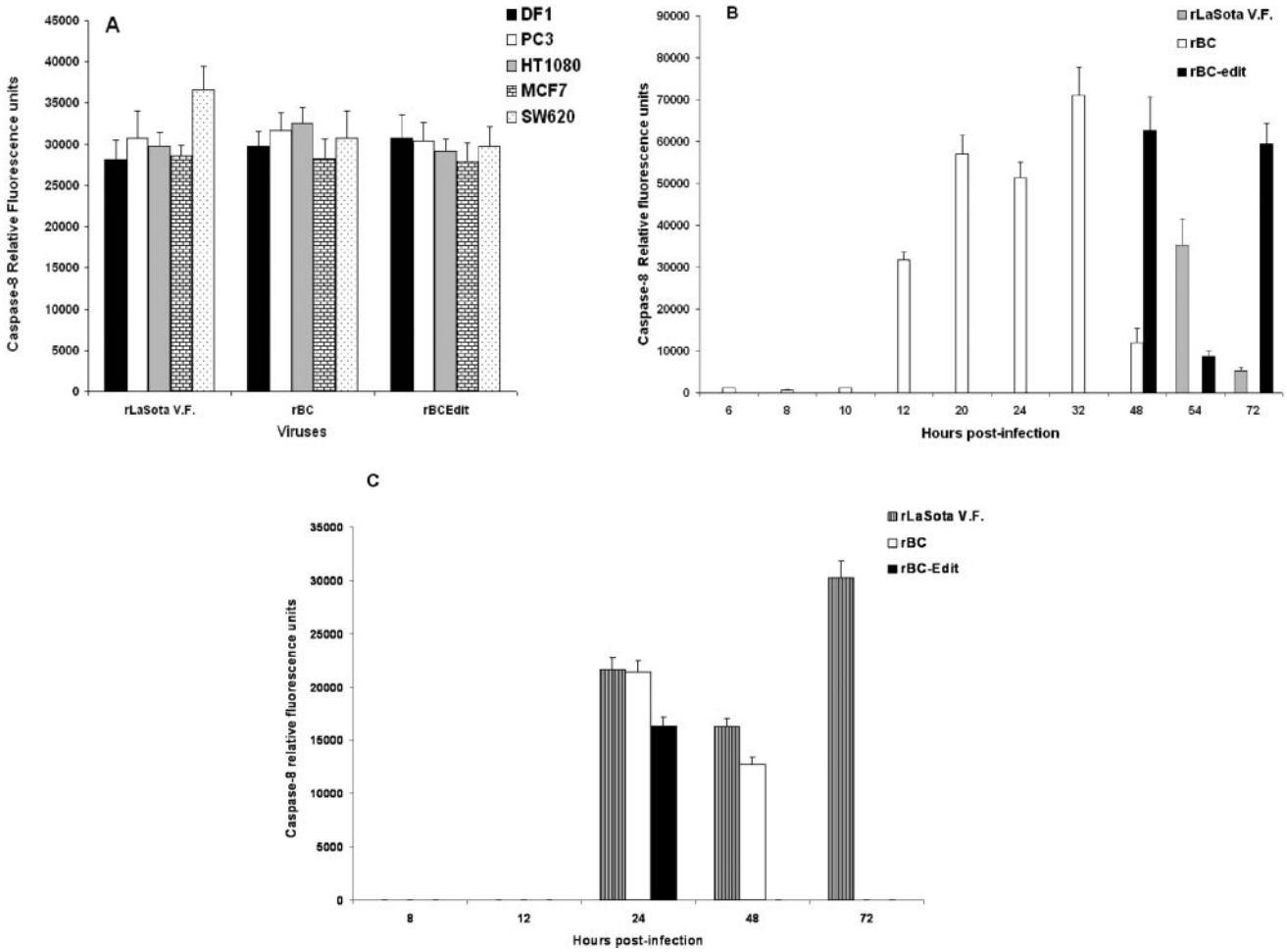

FIG. 4. Caspase-8 expression in NDV-induced apoptosis of tumor cells. DF1 and various human tumor cells were either mock infected or infected with rLaSota V.F., rBC, or rBC-Edit strains of NDV at an MOI of 0.01. Culture supernatants were assayed by ELISA for caspase-8 production at 48 h postinfection. The relative fluorescence units over mock-infected controls are shown for DF1 and a few representative human tumor cells for caspase-8 (A). (B) Kinetics of caspase-8 induction in HuTu80 cells. (C) Caspase-8 production in caspase-8-methylated SH-SY5Y neuroblastoma cells. Results represent mean values + SEM from two independent experiments.

NDV-induced apoptosis is caspase dependent. To identify whether rNDV-induced apoptosis is entirely dependent on caspase activation, HuTu80 epithelial cells were pretreated with the broad-specificity caspase inhibitor Z-VAD-FMK or with relatively specific inhibitors of caspase-9 (Z-LEHD-FMK), caspase-3 (Z-DEVD-FMK), and caspase-8 (Z-IETD-FMK) and infected with rBC-EGFP. The expression of EGFP was monitored by epifluorescence microscopy, and virus content in the supernatant was determined by a plaque assay on DF1 cells at specified intervals. The broad-specificity caspase inhibitor Z-VAD-FMK was able to inhibit rNDV-triggered cytolysis completely until 48 h p.i., indicating that NDV-mediated cytotoxicity is caspase dependent. But after 48 h p.i., CPE appeared in the form of syncytia and cell rounding, indicating that rNDV can also induce caspase-independent lysis, perhaps as a direct result of viral replication. An intranucleosomal DNA fragmentation assay of infected cells confirmed apoptosis. Furthermore, despite the block in apoptosis, titers of infectious virus in Z-VAD-FMK-treated cells were similar to those in untreated cells (Fig. 7D), which implies that apoptosis is not required by the virus as a mechanism to facilitate its replication. Caspase-8 and caspase-9 inhibitors also suppressed morphological and biochemical alteration of NDV-infected cells until 48 h p.i. But none of them were able to individually protect HuTu80 cells from rNDV-induced apoptosis, which suggests that rNDV triggers multiple caspase-dependent pathways in these cells. From the above results, we infer that NDV triggers apoptosis by a rapid dissociation of the mitochondrial membrane potential, the release of cytochrome *c*, and the activation of caspase-9. Further, we detected caspase-8 late in the infection cycle, suggesting that multiple pathways that lead to the death of NDV-infected cells could be acting after an initial proapoptotic signal subsequent to the entry of the virus.

DISCUSSION

The genetic malleability and inherent tumor selectivity of NDV afford the opportunity to enhance its therapeutic potential. With the advent of reverse genetic systems for NDV, it is now possible to refine and optimize the oncolytic potency,

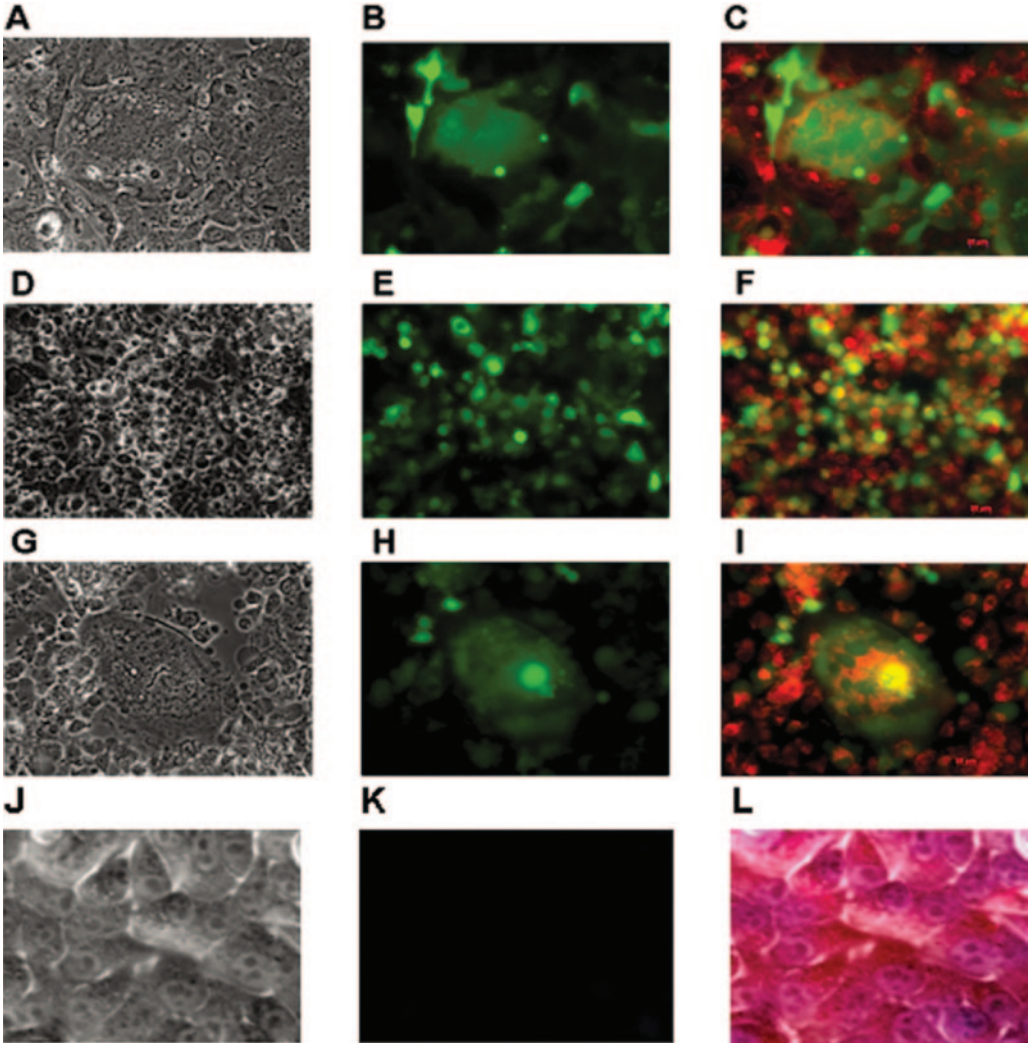

FIG. 5. Disruption of mitochondrial membrane potential in rBC-EGFP-infected tumor cells was examined by staining with DAPI and MitoTracker Red CMX-Ros. NDV-infected cells which had a disruption of the $\Delta\psi_m$ and were undergoing apoptosis were shown by the diffuse cytoplasmic pattern of CMX-Ros with condensed chromatin. Tumor cells were infected with rBC-EGFP virus, treated 24 h postinfection with MitoTracker Red CMX-Ros for 2 h, and fixed later. Syncytium formation, EGFP expression, and mitochondrial membrane disruption in rBC-EGFP-infected cells are shown. (A) CaCo2 colon carcinoma cells, bright field; magnification, ×40. (B) Epifluorescence microscopy, ×40. (C) Diffuse staining of cytoplasm with MitoTracker Red merged with fluorescent image, ×40. (D) HEpG2 hepatocarcinoma cells, bright field, ×40. (E) Epifluorescence, ×40. (F) Diffuse cytoplasmic staining of MitoTracker Red with EGFP expression, ×40. (G) PC3 prostate cancer cells, bright field, ×40. (H) Epifluorescence, ×40. (I) Diffuse cytoplasmic staining of MitoTracker Red with EGFP expression, ×40. (J) HuTu80 cells, uninfected control cells, bright field, ×40. (K) Epifluorescence, ×40. (L) Punctuate cytoplasmic staining with MitoTracker Red, ×40.

specificity, and therapeutic index, besides specifically retargeting it to the desired tumor cells. However, the exact modes of tumor cell killing by NDV are still incompletely understood. Understanding these mechanisms is crucial to improving oncolytic efficacy. Keeping this in mind, we explored the molecular mechanisms of oncolysis by rNDV. In order to achieve this, we examined the oncolytic potential of rNDVs with deficiencies in replicative abilities, cell and tissue tropism, and interferon antagonism. In addition, we engineered an rNDV with a reporter (EGFP) gene to make it possible to monitor virus infection. We have demonstrated that human tumor cells of neuroectodermal, mesenchymal, and epithelial origins could be infected and lysed by rNDV.

A nonpathogenic NDV (rLaSota V.F.) with a modified fusion protein cleavage site showed cytotoxicity against a wide range of tumor cells (86%), while a moderately pathogenic NDV (rBC) was cytolytic in only 57% of the tested tumor cells. However, the rBC virus efficiently lysed tumor cells at a relatively lower MOI. Engineering an additional transgene in rBC virus did not lower its oncolytic efficacy, as the cytotoxic range and effective concentration to lyse tumor cells of rBC and rBC-EGFP viruses were similar. But, the rLaSota V.F. and rBC viruses differed in their cytotoxic abilities against tumor cells, despite having similar F protein cleavage site sequences. We have previously shown that they also differ in virulence in chickens, the natural host for these viruses (41). Therefore, the observed differences in tumor cell cytotoxicity might be a reflection of the differences in the other major surface glycopro-

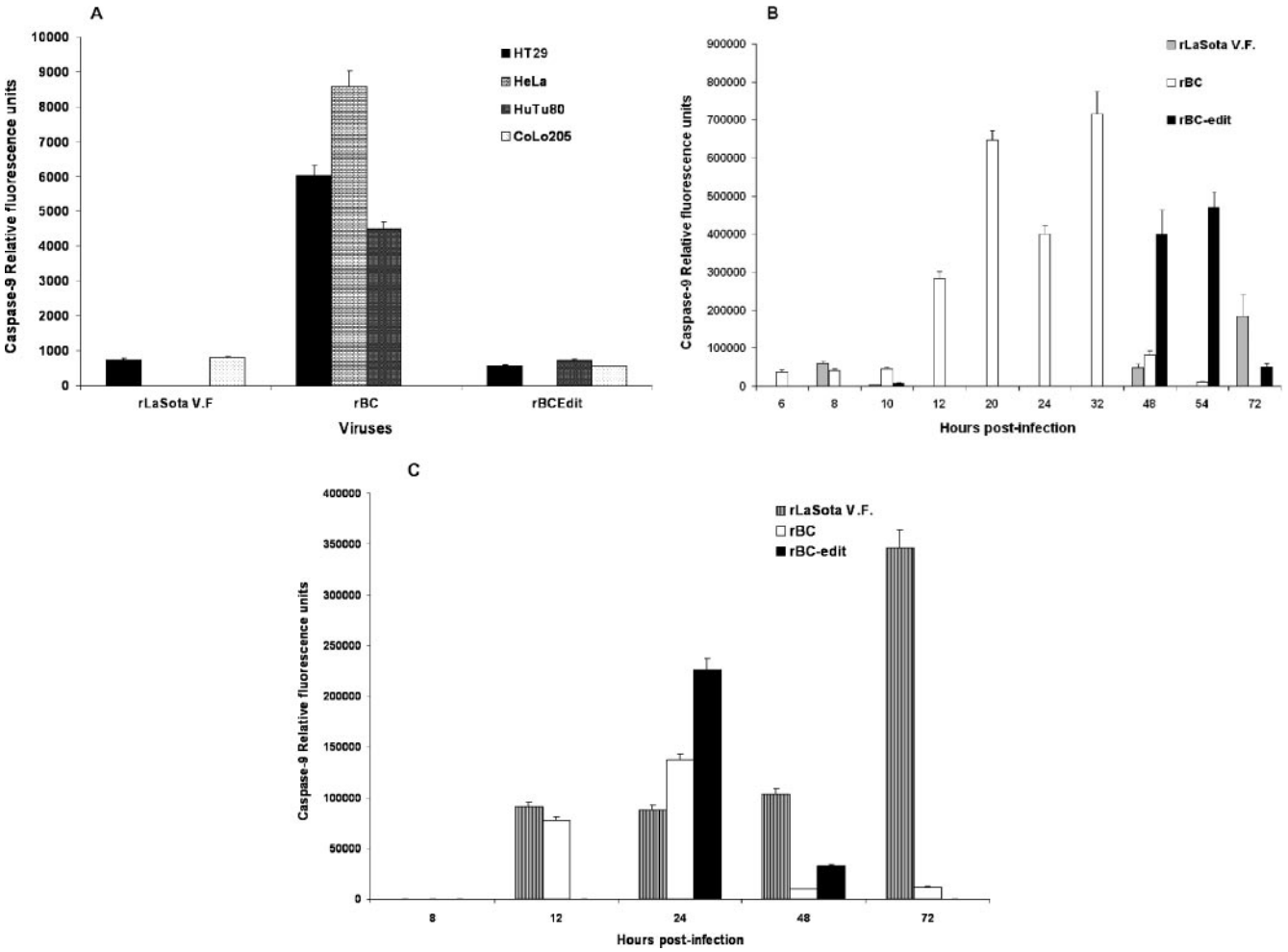

FIG. 6. Caspase-9 expression in NDV-induced apoptosis of tumor cells. DF1 and various human tumor cells were either mock infected or infected with rLaSota V.F., rBC, or rBC-Edit strains of NDV at an MOI of 0.01. Culture supernatants were assayed by ELISA for caspase-9 production at 48 h postinfection. (A) The relative fluorescence units over mock-infected controls are shown for DF1 cells and a few representative human tumor cells for caspase-9. (B) Kinetics of caspase-9 production in HuTu80 cells. (C) Caspase-9 production in SH-SY5Y neuroblastoma cells. Results represent mean values + SEM from two independent experiments.

tein, the HN protein. The HN protein has been shown to mediate apoptosis in NDV-infected cells (63). There are 17 amino acid differences in the HN protein between rLaSota and rBC viruses that might contribute to these differences. Since all strains of NDV enter all types of cells using sialic acid receptors, the observed differences in cytotoxicity against tumor cells by these viruses are likely due to other HN protein functional differences that do not alter receptor specificity. It is highly likely that these differences could be due to a difference in receptor avidity resulting from the amino acid differences in the HN protein. It is also possible that other viral proteins, such as the V and L proteins, may be responsible for these differences. The rBC-Edit virus, on the other hand, showed a wider spectrum of cytotoxicity with a very low MOI. This could be due to the absence of expression of the V protein, which is reported to be an antiapoptotic protein (42).

NDV has been reported to induce apoptosis in infected cells (12, 27, 63), which is considered to be mediated by TRAIL (58). Mitogen-activated protein kinase pathways or reactive oxygen species are not associated with apoptosis induced by NDV (12). However, the exact cellular pathways of NDV-induced apoptosis and the mechanistic basis of oncolysis are largely unknown. By using an array of tumor cells defective in components of apoptotic machinery and IFN signaling, we have shown that NDV mediates tumor cell killing independently of IFN signaling by using multiple caspase-mediated apoptotic pathways. The inability to execute cell death in caspase-3 null MCF-7 cells reinforces our claim that NDV is oncolytic only by caspase-dependent apoptosis. The process of mitochondrial outer membrane permeabilization leading to the leakage of cytochrome *c* and probably other proteins, including Smac, from the intermembrane space (IMS) and the factors that regulate this process following rNDV-induced apoptosis remain to be discerned. The redistribution of these particular IMS proteins may be triggered by events upstream of the mitochondria, such as Bax recruitment to the outer mitochondrial membrane. Additionally, feed-forward loops external to mitochondria, such as those involving Ca^{2+} release

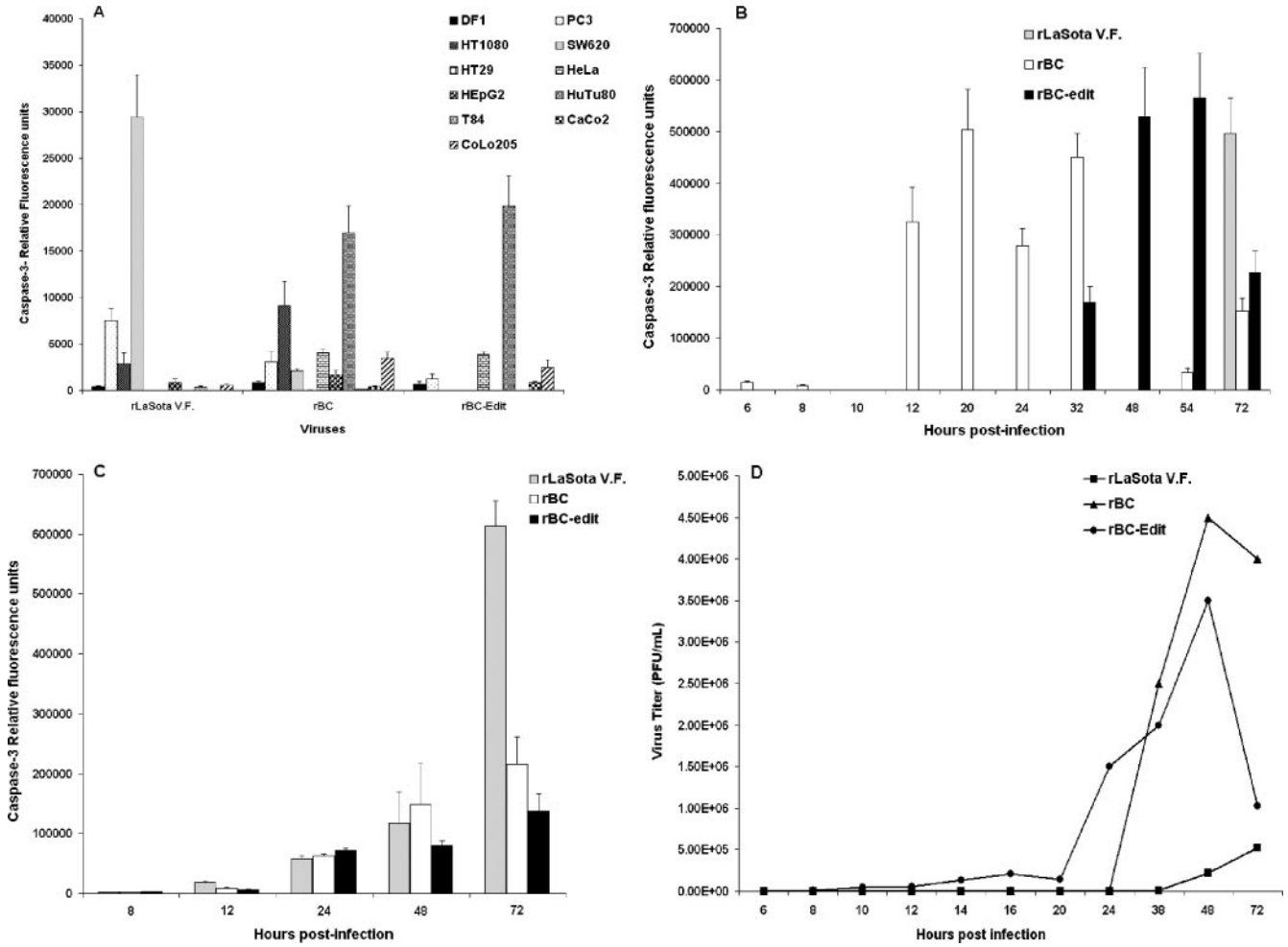

FIG. 7. Effector caspase-3 expression in NDV-induced apoptosis of tumor cells. DF1 and various human tumor cells were either mock infected or infected with rLaSota V.F., rBC, or rBC-Edit strains of NDV at an MOI of 0.01. Culture supernatants were assayed by ELISA for caspase-3 production at 48 h postinfection. (A) The relative fluorescence units over mock-infected controls are shown for DF1 and a few representative human tumor cells for caspase-3. (B) Kinetics of caspase-3 production in HuTu80 cells. (C) Caspase-3 production in SH-SY5Y neuroblastoma cells. Results represent mean values + SEM from two independent experiments. Broad-spectrum caspase inhibitor does not prevent replication of NDV in human tumor cells. HuTu80 cells were pretreated for 1 h with 100 μM Z-VAD-FMK prior to infection with rLaSota V.F., rBC, or rBC-Edit (MOI = 1) virus or mock infection. Virus content in the supernatant of infected cells was assayed by a plaque assay in DF1 cells at the indicated time points postinfection (D). Virus titers in control cells with dimethyl sulfoxide treatment were not significantly different ($P > 0.05$). Results represent mean values + SEM from two independent experiments.

from endoplasmic reticulum, may act to coordinate the entire population of mitochondria in one cell to release cytochrome *c* and other IMS proteins (5, 33).

The most proximal event in NDV-mediated apoptosis is the activation of caspase-9, followed by the activation of caspase-3, and ultimately the activation of caspase-8. Given that caspase-8 was originally identified as an initiator caspase triggered by death receptors, its involvement as a late event in NDV-induced apoptosis was unanticipated. The sequence of caspase activation we observed suggests activation of caspase-8 via caspase-3, which in turn may be triggered by the mitochondrial pathway via caspase-9. Once activated, caspase-8 may participate in an amplification mechanism, further activating effector caspases to accelerate NDV-mediated cell death. Indeed, recent studies have shown the ability of chemotherapeutic drugs to elicit the processing of caspase-8 in the absence of CD95 ligand-receptor interaction, and caspase-8 activation can occur downstream of caspase-9 and caspase-3 in response to anticancer drugs (60–61). In this regard, pathways of apoptosis induced by NDV overlap those induced by DNA-damaging chemotherapeutic drugs. NDV causes the loss of mitochondrial membrane potential both in wild-type cells and in cells devoid of functional caspase-8. Inhibition of caspase-8 activation, as in neuroblastoma cells, or TRAIL resistance, as in HT29 and CaCo2 cells (29), did not alter the apoptotic events in these cells. Despite TRAIL resistance, we were able to demonstrate that the rBC-Edit virus and the rLaSota V.F. virus were apoptotic in HT29 and CaCo2 cells, but the rBC virus is noncytolytic in these cells, probably due to the potent antiapoptotic activity of the V protein. These results confirm our findings that NDV-induced TRAIL potentiates only the intrinsic apoptotic pathway.

As reported for vesicular stomatitis virus (1, 15), we also found that caspase-8 and caspase-9 inhibitors did not completely abrogate the signs of apoptosis in NDV-infected cells and that the presence of the general caspase inhibitor Z-VAD-FMK during the infection cycle prevented apoptosis and delayed cell death but could not inhibit CPE induced by the virus after 48 h p.i. In addition, we found that the activation of caspases in NDV-infected cells is not a requirement for viral replication, since caspase inhibitors had no effect on virus replication. These data show that NDV kills cancer cells primarily by activation of the mitochondrial death pathway, and furthermore, they indicate that the caspase-8/Bid-dependent signal amplification loop is not important for NDV-induced death. Viruses that induce death receptor-dependent apoptosis include human immunodeficiency virus (38), measles virus (57), influenza A virus (40), Sindbis virus (16), reovirus (9), lyssavirus (23), and hepatitis C virus (2). A number of viruses have been found to cause relocalization of proapoptotic mitochondrial proteins into the cytosol. Among these are human immunodeficiency virus (13), influenza A virus (7), herpes simplex virus type 1 (64), herpes simplex virus type 8 (49), hepatitis B virus (54), reovirus (24), and West Nile virus (43).

Our data identify the mechanistic events leading to apoptosis when tumor cells are infected with NDV. We have demonstrated that apoptosis is initiated by rNDV through the mitochondrial intrinsic pathway, leading to the activation of caspase-9 and effector caspase-3. A second round of caspase activation occurs when TRAIL-induced death receptor-mediated or caspase-3-mediated caspase-8 activation commences. Caspase-8 amplifies the cycle, allowing full expression of apoptosis leading to oncolysis. While caspase-8 may play a role in amplifying effector caspase activation, this appears to be unnecessary for NDV-induced apoptosis. The delay in TRAIL expression also supports this view. Reoviruses induce apoptosis primarily through the death receptor pathway, and cytochrome *c* release and subsequent caspase-9 activation were not critical mitochondrial events in apoptosis induction (24). NDV, on the other hand, depends primarily on the mitochondrial apoptotic pathway with no dependence on the death receptor pathway, which suggests that the molecular mechanisms of apoptosis may depend on the virus strain and cell type.

We have also shown that reporter genes could be engineered in rNDV to track the sojourn of oncolytic virus in the host without diminishing its oncolytic efficacy. The rLaSota V.F. and rBC-Edit viruses reported here have a number of properties which make them suitable as oncolytic viruses for tumor therapy. (i) These viruses are nonpathogenic to humans. We therefore hypothesize that they will be associated with fewer side effects. In fact, our recent studies in nonhuman primates showed that rNDV undergoes only a limited replication in the lungs with no clinical effects (6). (ii) Multiple serologically defined types exist for avian paramyxoviruses (APMV); different serotypes (APMV-2 to APMV-9) can therefore be engineered to deliver therapeutic transgenes. Alternatively, rNDV (APMV-1) with different antigenic specificity could be constructed by exchanging the surface glycoproteins of the virus from serotypes APMV-2 to -9. Therefore, immunity of the host after the first round of rNDV therapy can be circumvented by choosing rNDV with appropriate surface glycoproteins or recombinant APMV of differing serotypes, allowing repeated administration. (iii) It is possible to construct rNDVs with multiple transgenes to enhance oncolytic efficacy, as NDV has been shown to accommodate up to 4 kb of foreign genes. (iv) These viruses could be engineered for targeting to specific sites.

ACKNOWLEDGMENTS

We thank Zhuhui Huang, Peter Savage, Govindarajan Dhanasekaran, and Subrat Rout for technical help.

REFERENCES

1. **Balachandran, S., M. Porosnicu, and G. N. Barber.** 2001. Oncolytic activity of vesicular stomatitis virus is effective against tumors exhibiting aberrant p53, Ras, or myc function and involves the induction of apoptosis. J. Virol. **75:**3474–3479.
2. **Balasubramanian, A., M. Koziel, J. E. Groopman, and R. K. Ganju.** 2005. Molecular mechanism of hepatic injury in coinfection with hepatitis C virus and HIV. Clin. Infect. Dis. **41**(Suppl. 1)**:**S32–S37.
3. **Bell, J. C., K. A. Garson, B. D. Lichty, and D. F. Stojdl.** 2002. Oncolytic viruses: programmable tumour hunters. Curr. Gene Ther. **2:**243–254.
4. **Bian, H., P. Fournier, B. Peeters, and V. Schirrmacher.** 2005. Tumor-targeted gene transfer in vivo via recombinant Newcastle disease virus modified by a bispecific fusion protein. Int. J. Oncol. **27:**377–384.
5. **Boehning, D., R. L. Patterson, L. Sedaghat, N. O. Glebova, T. Kurosaki, and S. H. Snyder.** 2003. Cytochrome c binds to inositol (1,4,5) trisphosphate receptors, amplifying calcium-dependent apoptosis. Nat. Cell Biol. **5:**1051–1061.
6. **Bukreyev, A., Z. Huang, L. Yang, S. Elankumaran, M. St Claire, B. R. Murphy, S. K. Samal, and P. L. Collins.** 2005. Recombinant Newcastle disease virus expressing a foreign viral antigen is attenuated and highly immunogenic in primates. J. Virol. **79:**13275–13284.
7. **Chen, W., P. A. Calvo, D. Malide, J. Gibbs, U. Schubert, I. Bacik, S. Basta, R. O'Neill, J. Schickli, P. Palese, P. Henklein, J. R. Bennink, and J. W. Yewdell.** 2001. A novel influenza A virus mitochondrial protein that induces cell death. Nat. Med. **7:**1306–1312.
8. **Choppin, P. W., and A. Scheid.** 1980. The role of viral glycoproteins in adsorption, penetration, and pathogenicity of viruses. Rev. Infect. Dis. **2:**40–61.
9. **Clarke, P., S. M. Meintzer, S. Gibson, C. Widmann, T. P. Garrington, G. L. Johnson, and K. L. Tyler.** 2000. Reovirus-induced apoptosis is mediated by TRAIL. J. Virol. **74:**8135–8139.
10. **Csatary, L. K.** 1971. Viruses in the treatment of cancer. Lancet **2:**825.
11. **Du, C., M. Fang, Y. Li, L. Li, and X. Wang.** 2000. Smac, a mitochondrial protein that promotes cytochrome c-dependent caspase activation by eliminating IAP inhibition. Cell **102:**33–42.
12. **Fabian, Z., B. Torocsik, K. Kiss, L. K. Csatary, B. Bodey, J. Tigyi, C. Csatary, and J. Szeberenyi.** 2001. Induction of apoptosis by a Newcastle disease virus vaccine (MTH-68/H) in PC12 rat phaeochromocytoma cells. Anticancer Res. **21:**125–135.
13. **Ferri, K. F., E. Jacotot, J. Blanco, J. A. Este, and G. Kroemer.** 2000. Mitochondrial control of cell death induced by HIV-1-encoded proteins. Ann. N. Y. Acad. Sci. **926:**149–164.
14. **Fulda, S., W. Wick, M. Weller, and K. M. Debatin.** 2002. Smac agonists sensitize for Apo2L/TRAIL- or anticancer drug-induced apoptosis and induce regression of malignant glioma in vivo. Nat. Med. **8:**808–815.
15. **Gadaleta, P., X. Perfetti, S. Mersich, and F. Coulombie.** 2005. Early activation of the mitochondrial apoptotic pathway in vesicular stomatitis virus-infected cells. Virus Res. **109:**65–69.
16. **Griffin, D. E.** 2005. Neuronal cell death in alphavirus encephalomyelitis. Curr. Top. Microbiol. Immunol. **289:**57–77.
17. **Hu, S., C. Vincenz, M. Buller, and V. M. Dixit.** 1997. A novel family of viral death effector domain-containing molecules that inhibit both CD-95- and tumor necrosis factor receptor-1-induced apoptosis. J. Biol. Chem. **272:**9621–9624.
18. **Huang, Z., S. Krishnamurthy, A. Panda, and S. K. Samal.** 2001. High-level expression of a foreign gene from the most 3′-proximal locus of a recombinant Newcastle disease virus. J. Gen. Virol. **82:**1729–1736.
19. **Huang, Z., S. Krishnamurthy, A. Panda, and S. K. Samal.** 2003. Newcastle disease virus V protein is associated with viral pathogenesis and functions as an alpha interferon antagonist. J. Virol. **77:**8676–8685.
20. **Ichikawa, K., W. Liu, L. Zhao, Z. Wang, D. Liu, T. Ohtsuka, H. Zhang, J. D. Mountz, W. J. Koopman, R. P. Kimberly, and T. Zhou.** 2001. Tumoricidal activity of a novel anti-human DR5 monoclonal antibody without hepatocyte cytotoxicity. Nat. Med. **7:**954–960.
21. **Igney, F. H., and P. H. Krammer.** 2002. Death and anti-death: tumour resistance to apoptosis. Nat. Rev. Cancer **2:**277–288.
22. **Johnsen, J. I., I. Pettersen, F. Ponthan, B. Sveinbjornsson, T. Flaegstad, and P. Kogner.** 2004. Synergistic induction of apoptosis in neuroblastoma cells using a combination of cytostatic drugs with interferon-gamma and TRAIL. Int. J. Oncol. **25:**1849–1857.

23. **Kassis, R., F. Larrous, J. Estaquier, and H. Bourhy.** 2004. Lyssavirus matrix protein induces apoptosis by a TRAIL-dependent mechanism involving caspase-8 activation. J. Virol. **78:**6543–6555.
24. **Kominsky, D. J., R. J. Bickel, and K. L. Tyler.** 2002. Reovirus-induced apoptosis requires both death receptor- and mitochondrial-mediated caspase-dependent pathways of cell death. Cell Death Differ. **9:**926–933.
25. **Krammer, P. H.** 1999. CD95(APO-1/Fas)-mediated apoptosis: live and let die. Adv. Immunol. **71:**163–210.
26. **Krishnamurthy, S., Z. Huang, and S. K. Samal.** 2000. Recovery of a virulent strain of Newcastle disease virus from cloned cDNA: expression of a foreign gene results in growth retardation and attenuation. Virology **278:**168–182.
27. **Krishnamurthy, S., and S. K. Samal.** 1998. Nucleotide sequences of the trailer, nucleocapsid protein gene and intergenic regions of Newcastle disease virus strain Beaudette C and completion of the entire genome sequence. J. Gen. Virol. **79:**2419–2424.
28. **Kruyt, F. A., and D. T. Curiel.** 2002. Toward a new generation of conditionally replicating adenoviruses: pairing tumor selectivity with maximal oncolysis. Hum. Gene Ther. **13:**485–495.
29. **Lacour, S., A. Hammann, A. Wotawa, L. Corcos, E. Solary, and M. T. Dimanche-Boitrel.** 2001. Anticancer agents sensitize tumor cells to tumor necrosis factor-related apoptosis-inducing ligand-mediated caspase-8 activation and apoptosis. Cancer Res. **61:**1645–1651.
30. **Lam, K. M., A. C. Vasconcelos, and A. A. Bickford.** 1995. Apoptosis as a cause of death in chicken embryos inoculated with Newcastle disease virus. Microb. Pathog. **19:**169–174.
31. **Lana, D. P., D. B. Snyder, D. J. King, and W. W. Marquardt.** 1988. Characterization of a battery of monoclonal antibodies for differentiation of Newcastle disease virus and pigeon paramyxovirus-1 strains. Avian Dis. **32:** 273–281.
32. **Li, L., R. M. Thomas, H. Suzuki, J. K. De Brabander, X. Wang, and P. G. Harran.** 2004. A small molecule Smac mimic potentiates TRAIL- and TNFalpha-mediated cell death. Science **305:**1471–1474.
33. **Lim, M. L., B. Chen, P. M. Beart, and P. Nagley.** 2006. Relative timing of redistribution of cytochrome c and Smac/DIABLO from mitochondria during apoptosis assessed by double immunocytochemistry on mammalian cells. Exp. Cell Res. **312:**1174–1184.
34. **Lorence, R. M., B. B. Katubig, K. W. Reichard, H. M. Reyes, A. Phuangsab, M. D. Sassetti, R. J. Walter, and M. E. Peeples.** 1994. Complete regression of human fibrosarcoma xenografts after local Newcastle disease virus therapy. Cancer Res. **54:**6017–6021.
35. **Lorence, R. M., K. W. Reichard, B. B. Katubig, H. M. Reyes, A. Phuangsab, B. R. Mitchell, C. J. Cascino, R. J. Walter, and M. E. Peeples.** 1994. Complete regression of human neuroblastoma xenografts in athymic mice after local Newcastle disease virus therapy. J. Natl. Cancer Inst. **86:**1228–1233.
36. **Lorence, R. M., P. A. Rood, and K. W. Kelley.** 1988. Newcastle disease virus as an antineoplastic agent: induction of tumor necrosis factor-alpha and augmentation of its cytotoxicity. J. Natl. Cancer Inst. **80:**1305–1312.
37. **Mayo, M. A.** 2002. A summary of taxonomic changes recently approved by ICTV. Arch. Virol. **147:**1655–1666.
38. **Miura, Y., N. Misawa, N. Maeda, Y. Inagaki, Y. Tanaka, M. Ito, N. Kayagaki, N. Yamamoto, H. Yagita, H. Mizusawa, and Y. Koyanagi.** 2001. Critical contribution of tumor necrosis factor-related apoptosis-inducing ligand (TRAIL) to apoptosis of human CD4+ T cells in HIV-1-infected hu-PBL-NOD-SCID mice. J. Exp. Med. **193:**651–660.
39. **Nagata, S.** 1997. Apoptosis by death factor. Cell **88:**355–365.
40. **Nichols, J. E., J. A. Niles, and N. J. Roberts, Jr.** 2001. Human lymphocyte apoptosis after exposure to influenza A virus. J. Virol. **75:**5921–5929.
41. **Panda, A., Z. Huang, S. Elankumaran, D. D. Rockemann, and S. K. Samal.** 2004. Role of fusion protein cleavage site in the virulence of Newcastle disease virus. Microb. Pathog. **36:**1–10.
42. **Park, M. S., M. L. Shaw, J. Munoz-Jordan, J. F. Cros, T. Nakaya, N. Bouvier, P. Palese, A. Garcia-Sastre, and C. F. Basler.** 2003. Newcastle disease virus (NDV)-based assay demonstrates interferon-antagonist activity for the NDV V protein and the Nipah virus V, W, and C proteins. J. Virol. **77:**1501–1511.
43. **Parquet, M. C., A. Kumatori, F. Hasebe, K. Morita, and A. Igarashi.** 2001. West Nile virus-induced bax-dependent apoptosis. FEBS Lett. **500:**17–24.
44. **Phuangsab, A., R. M. Lorence, K. W. Reichard, M. E. Peeples, and R. J. Walter.** 2001. Newcastle disease virus therapy of human tumor xenografts: antitumor effects of local or systemic administration. Cancer Lett. **172:**27–36.
45. **Pokrovskaja, K., T. Panaretakis, and D. Grander.** 2005. Alternative signaling pathways regulating type I interferon-induced apoptosis. J. Interferon Cytokine Res. **25:**799–810.
46. **Rathmell, J. C., and C. B. Thompson.** 1999. The central effectors of cell death in the immune system. Annu. Rev. Immunol. **17:**781–828.
47. **Reichard, K. W., R. M. Lorence, C. J. Cascino, M. E. Peeples, R. J. Walter, M. B. Fernando, H. M. Reyes, and J. A. Greager.** 1992. Newcastle disease virus selectively kills human tumor cells. J. Surg. Res. **52:**448–453.
48. **Sangfelt, O., S. Erickson, J. Castro, T. Heiden, S. Einhorn, and D. Grander.** 1997. Induction of apoptosis and inhibition of cell growth are independent responses to interferon-alpha in hematopoietic cell lines. Cell Growth Differ. **8:**343–352.
49. **Sharp, T. V., H. W. Wang, A. Koumi, D. Hollyman, Y. Endo, H. Ye, M. Q. Du, and C. Boshoff.** 2002. K15 protein of Kaposi's sarcoma-associated herpesvirus is latently expressed and binds to HAX-1, a protein with antiapoptotic function. J. Virol. **76:**802–816.
50. **Steward, M., I. B. Vipond, N. S. Millar, and P. T. Emmerson.** 1993. RNA editing in Newcastle disease virus. J. Gen. Virol. **74:**2539–2547.
51. **Stojdl, D. F., B. Lichty, S. Knowles, R. Marius, H. Atkins, N. Sonenberg, and J. C. Bell.** 2000. Exploiting tumor-specific defects in the interferon pathway with a previously unknown oncolytic virus. Nat. Med. **6:**821–825.
52. **Szeberenyi, J., Z. Fabian, B. Torocsik, K. Kiss, and L. K. Csatary.** 2003. Newcastle disease virus-induced apoptosis in PC12 pheochromocytoma cells. Am. J. Ther. **10:**282–288.
53. **Teitz, T., T. Wei, M. B. Valentine, E. F. Vanin, J. Grenet, V. A. Valentine, F. G. Behm, A. T. Look, J. M. Lahti, and V. J. Kidd.** 2000. Caspase 8 is deleted or silenced preferentially in childhood neuroblastomas with amplification of MYCN. Nat. Med. **6:**529–535.
54. **Terradillos, O., A. de La Coste, T. Pollicino, C. Neuveut, D. Sitterlin, H. Lecoeur, M. L. Gougeon, A. Kahn, and M. A. Buendia.** 2002. The hepatitis B virus X protein abrogates Bcl-2-mediated protection against Fas apoptosis in the liver. Oncogene **21:**377–386.
55. **Thornberry, N. A., and Y. Lazebnik.** 1998. Caspases: enemies within. Science **281:**1312–1316.
56. **Verhagen, A. M., P. G. Ekert, M. Pakusch, J. Silke, L. M. Connolly, G. E. Reid, R. L. Moritz, R. J. Simpson, and D. L. Vaux.** 2000. Identification of DIABLO, a mammalian protein that promotes apoptosis by binding to and antagonizing IAP proteins. Cell **102:**43–53.
57. **Vidalain, P. O., O. Azocar, B. Lamouille, A. Astier, C. Rabourdin-Combe, and C. Servet-Delprat.** 2000. Measles virus induces functional TRAIL production by human dendritic cells. J. Virol. **74:**556–559.
58. **Washburn, B., M. A. Weigand, A. Grosse-Wilde, M. Janke, H. Stahl, E. Rieser, M. R. Sprick, V. Schirrmacher, and H. Walczak.** 2003. TNF-related apoptosis-inducing ligand mediates tumoricidal activity of human monocytes stimulated by Newcastle disease virus. J. Immunol. **170:**1814–1821.
59. **Weaver, B. K., O. Ando, K. P. Kumar, and N. C. Reich.** 2001. Apoptosis is promoted by the dsRNA-activated factor (DRAF1) during viral infection independent of the action of interferon or p53. FASEB J. **15:**501–515.
60. **Wesselborg, S., I. H. Engels, E. Rossmann, M. Los, and K. Schulze-Osthoff.** 1999. Anticancer drugs induce caspase-8/FLICE activation and apoptosis in the absence of CD95 receptor/ligand interaction. Blood **93:**3053–3063.
61. **Wieder, T., F. Essmann, A. Prokop, K. Schmelz, K. Schulze-Osthoff, R. Beyaert, B. Dorken, and P. T. Daniel.** 2001. Activation of caspase-8 in drug-induced apoptosis of B-lymphoid cells is independent of CD95/Fas receptor-ligand interaction and occurs downstream of caspase-3. Blood **97:** 1378–1387.
62. **Wilson, M. R.** 1998. Apoptotic signal transduction: emerging pathways. Biochem. Cell Biol. **76:**573–582.
63. **Zeng, J., P. Fournier, and V. Schirrmacher.** 2002. Induction of interferon-alpha and tumor necrosis factor-related apoptosis-inducing ligand in human blood mononuclear cells by hemagglutinin-neuraminidase but not F protein of Newcastle disease virus. Virology **297:**19–30.
64. **Zhou, G., and B. Roizman.** 2000. Wild-type herpes simplex virus 1 blocks programmed cell death and release of cytochrome *c* but not the translocation of mitochondrial apoptosis-inducing factor to the nuclei of human embryonic lung fibroblasts. J. Virol. **74:**9048–9053.
65. **Zorn, U., I. Dallmann, J. Grosse, H. Kirchner, H. Poliwoda, and J. Atzpodien.** 1994. Induction of cytokines and cytotoxicity against tumor cells by Newcastle disease virus. Cancer Biother. **9:**225–235.